5 Dissolution of Milled Minerals in Dilute Acid

5.1 Introduction

Attrition milling of silicate minerals is shown in the previous chapter to decrease particle size and increase the specific surface area of minerals. Surface dislocations produced by grinding increase dissolution rates (Holdren and Speyer, 1985b) and Blum et al. (1990) proposes that the presence of dislocations on a mineral surface influences dissolution by (i) changing the overall thermodynamic properties and (ii) changing the kinetic mechanisms by which the material is removed from the surface. The role of ultrafine particles in the dissolution of ground minerals is not fully understood (Blum and Stillings, 1995) and the presence of ultrafine particles has been proposed as an explanation for the initial rapid dissolution of silicates prior to initiation of a slower long-term steady-state dissolution rate (Blum and Stillings, 1995; Holdren and Berner, 1979; Knauss et al., 1993). Great care is currently undertaken in dissolution experiments to remove this fine material (e.g. Welch et al., 1999) although Lee et al. (1998) caution against ultrasonic cleaning of mineral grains prior to experimental work as this may destroy features important to the mechanisms and rates of mineral dissolution. Other explanations for rapid initial dissolution have been proposed including disruption of the surface layer during grinding (Petrovic, 1981a; Petrovic, 1981b) in which case removal of the finest material will not change this mechnaism.

The silicate minerals subjected to high intensity attrition milling and characterised in the previous chapter provide an opportunity to determine factors affecting dissolution of ultrafine-grained material and evaluate the controls at the mineral surface. The very small particle size of minerals used in dissolution experiments, however, poses analytical problems for determinations of dissolved cations by spectroscopic techniques (flame photometry, AAS and ICP). Nanometric particulate matter passes through the finest filters and can not be removed by centrifugation (Menzies et al., 1992) and is ionised within the AAS flame or plasma, resulting in the overestimation of dissolved elements. Alternative analytical methods involving ion specific electrodes and colorimetric procedures lack sufficient sensitivity. Dialysis membranes will not transmit nanometre micro-particulates and have been used for separating particles and solutions when studying the speciation of trace metals and Al in fresh waters (Berggren, 1989; Borg, 1986). The use of dialysis

tubing to separate solid and solution has been limited in studies of dissolution reactions due to assumed long equilibration times (Lead et al., 1997), although a dialysis-cell reactor is described by Kalinowski and Schweda (1996). The dialysis method has been investigated here to determine its applicability for measuring dissolution kinetics of nanometre silicate minerals produced by attrition milling.

The principle aim of this chapter is to determine the influence of attrition milling on the reactivity of silicate minerals as determined by the release of major cations in deionised water and dilute acid solutions.

5.2 Materials and Methods

5.2.1 Dissolution Method

The minerals used in this experiment were those prepared in the SPEX mill (Section 3.2.2) and are described in Chapter 4. The experiment was designed to evaluate dissolution of milled minerals under two conditions. One set of subsamples was dissolved in deionised water to indicate changes that may occur in soil solution as a result of the addition of mineral fertilisers. The second solution consisted of deionised water adjusted to pH 4.5±0.1, which was then maintained at this pH throughout the experiment by adjusting pH daily with HCl. The solutions are referred throughout this paper as unbuffered and acid solutions, respectively. Pouches of dialysis tubing (Sigma Product D 9777) of an approximate pore size of 2.5nm, 25 cm in length, 25mm flat dry width, an average dry diameter of 16mm were prepared for each mineral. Each pouch received 0.25g of mineral and 25ml of solution, was sealed, and shaken by hand. The pouches were immersed in 500ml of appropriate solution and sealed in 500ml-polyethylene bottles that had been acid washed prior to use. The bottles were placed in an incubator on a horizontal orbital shaker table shaking at 100rpm and 40ºC. The bottles were placed horizontally to reduce settling of solids in the dialysis tubing.

Ten-ml solution aliquots were removed from each bottle after one day, and then at logarithmically increasing time periods. Leaking of minerals from the dialysis tubing was observed in several bottles between days 8 and 16, and the experiment halted after 16 days. Solutions and minerals within the dialysis tubing were collected at the end of the experiment and centrifuged at 11.5G for 5 minutes. An aliquot of solution was removed from the dialysis tubing and passed through a 0.22μm syringe filter prior to analysis.

The pH of the solution in each bottle was measured at the time of sampling. Each solution was analysed for Si using the molybdate blue method (Strickland and Parsons, 1968) and analysis for K (microcline, biotite), Mg (biotite, hornblende) and Ca (hornblende) by AAS and Na (microcline) by flame emission spectrometry. Insufficient volume was collected for analysis of Al.

5.2.2 Analysis of Data

Concentrations of dissolved elements were plotted against dissolution time and results are reported on a per unit mass basis for agronomic interpretation. Due to different shaped curves occurring in these plots, no single simple function closely describes all the data. Dissolution curves were described by the power equation used by Zhang and Bloom (1999) during studies of hornblende dissolution and following their convention:

$$E = aT^n \qquad \textit{Equation 5.1}$$

Where E is the cumulative elemental concentration (μmol g^{-1}) in solution, T is time (days) and a and n are constants. Coefficient a is a measure of the reactive sites on the surface based on unit mineral mass. Coefficient n describes the kinetics of the relationship and has been termed the reaction order by Zhang and Bloom (1999). Dissolution rates at each sampling time were calculated from the slope of the curve at time T by differentiation of the above equation:

$$\text{Rate} = \mathrm{d}E/\mathrm{d}T = anT^{n-1} \qquad \textit{Equation 5.2}$$

5.3 Results and Discussion

5.3.1 Dissolution Kinetics and Reaction Stoichiometry

Summary plots of elemental concentrations and corresponding solution stoichiometry are presented in *Figures 5.1* and *5.2* for microcline *Figures 5.3* and *5.4* for biotite and *Figures 5.6* and *5.7* for hornblende. The above power function has been used to describe the relationship between element concentration and time, although it is an approximation due to most curves being sigmoidal to some extent. Values of coefficients a (a measure of the density of reactive sites on the mineral surface) and n (the reaction order used to describe the relationship between elemental release and time) are presented in *Tables 5.1, 5.2* and

5.3. Values of *n* will be discussed in this section and values of *a* will be discussed in Section 5.3.2.

Microcline

Elemental concentrations of the bathing solution (*Figure 5.1*) were generally higher for milled minerals than for unmilled minerals and higher in the acid solution than in the deionised water. Concentrations also generally increased with milling time except for K release from M6 being greater than M24 in both solutions. While the reaction order *n* increased with milling time (*Table 5.1*), values of *n* for Si were higher than for K and Na, approximating 1 for Si dissolution of M6 and M24 in deionised water and 1.2 in acid solution. Values for K and Na were less than 0.8, except for K dissolution of M6 in acid solutions which was greater than 1 and larger than M24.

Table 5.1: Value of coefficients a (μmoles g^{-1}) and n of the power equation fitted to the relationship between cumulative element release and dissolution time for milled microcline in deionised water and acid (pH 4.5) solution. Values in brackets are the standard errors of the coefficients.

Element	Milling Time	Deionised Water			pH 4.5		
		a	*n*	R^2	*a*	*n*	R^2
Si	Initial	5.32 (±0.79)	0.81 (±0.06)	0.99	6.74 (±0.96)	0.72 (±0.06)	0.99
	1 hour	9.60 (±1.69)	0.87 (±0.07)	0.99	9.00 (±1.23)	0.88 (±0.05)	0.99
	6 hour	18.3 (±4.66)	1.05 (±0.10)	0.99	14.2 (±1.36)	1.20 (±0.04)	1.00
	24 hour	25.0 (±5.76)	1.03 (±0.09)	0.99	21.1 (±3.71)	1.23 (±0.07)	1.00
K	Initial	54.2 (±11.4)	0.06(±0.01)	0.76	14.3 (±1.78)	0.42 (±0.06)	0.97
	1 hour	49.8 (±15.8)	0.48 (±0.13)	0.88	31.8 (±8.17)	0.62 (±0.11)	0.95
	6 hour	54.7 (±22.3)	0.73 (±0.16)	0.92	23.6 (±1.61)	1.16 (±0.03)	1.00
	24 hour	45.0 (±13.2)	0.68 (±0.12)	0.95	55.2 (±21.5)	0.76 (±0.16)	0.94
Na	Initial	59.4 (±15.5)	0.00 (±0.16)	0.68	10.8 (±1.81)	0.52 (±0.07)	0.97
	1 hour	32.5 (±8.67)	0.37 (±0.12)	0.87	21.0 (±5.25)	0.52 (±0.11)	0.93
	6 hour	64.4 (±19.3)	0.56 (±0.12)	0.91	50.5 (±11.0)	0.69 (±0.09)	0.97
	24 hour	62.7 (±19.6)	0.56 (±0.13)	0.92	72.7 (±15.4)	0.64 (±0.09)	0.97

The rapid, initial release of K and Na relative to Si is also shown in the dissolution stoichiometry plots (*Figure 5.2a*). The K/Si and Na/Si ratios decrease with time, approaching congruent dissolution at day 16 of dissolution, by which time several percent of the mineral had dissolved. Most of this rapid, incongruent dissolution occurred during

dissolution of 1% of the mineral. The greater release of Na from feldspars has been reported in other dissolution experiments (Holdren and Berner, 1979; Wollast and Chou, 1985) for the rapid initial dissolution phase prior to development of steady-state, congruent dissolution. The initial release of K and Na from K feldspars has been attributed to the presence of compositional planes that are initiation points for dissolution and the presence of twinning (Lee et al., 1998). During the early stages of dissolution, solution composition may represent the composition of the high-strain-energy regions around the cores of dislocation outcrops (Lee and Parsons, 1995). The high K/Si and Na/Si ratios for initial dissolution decrease with milling time due to greater amounts of dissolution occurring (*Figure 5.2b*).

Biotite

Biotite dissolution (*Figure 5.3*) is associated with the release of K up to 30% of total K that can be attributed to rapid exchange of K^+ from the interlayer sites. The amount of quickly released K increased with increased milling time. Although the K^+ is exchanged with H^+ (Turpault and Trotignon, 1994), there is only a slight effect of pH on K dissolution, and this result is similar to results reported by Acker and Bricker (1992).

Si and Mg concentrations have been used to determine the rate of biotite dissolution with respect to the tetrahedral and octahedral layer respectively (Acker and Bricker, 1992; Turpault and Trotignon, 1994). Concentrations of both elements are greater in acid solutions than deionised water, especially Mg.

Reaction order for Si and Mg (*Table 5.2*) dissolution for B0 of about 0.5 indicates parabolic dissolution of both the tetrahedral and octahedral layer of the unmilled mineral in both solutions. The value for Si dissolution of B1 increased to approximately 1 in both solutions before decreasing for dissolution of B6 and B24, although differences in n may not be statistically significant. Mg reaction order increased for all milling times during dissolution in acid solutions and to B6 for dissolution in deionised water. Mg reaction order was approximately 1 for all samples except for B24 where $n \approx 1.4$. This suggests that the octahedral layer of highly milled biotite is easily dissolved in acid solution. Values of n for kinetics of K dissolution in both solutions are less than 0.3.

Table 5.2: Value of coefficients a (μmoles g^{-1}) and n of the power equation fitted to the relationship between cumulative element release and dissolution time for milled biotite in deionised water and acid (pH 4.5) solutions. Values in brackets are the standard errors of the coefficients.

Element	Milling Time	Deionised Water			pH 4.5		
		a	*n*	R^2	*a*	*n*	R^2
Si	Initial	18.6 (±2.76)	0.53 (±0.06)	0.98	16.3 (±3.01)	0.57 (±0.08)	0.97
	1 hour	28.0 (±6.74)	0.92 (±0.09)	0.98	24.0 (±4.67)	1.01 (±0.07)	0.99
	6 hour	41.3 (±8.15)	0.84 (±0.08)	0.99	60.1 (±6.99)	0.84 (±0.05)	0.99
	24 hour	39.2 (±8.06)	0.68 (±0.08)	0.97	38.0 (±5.76)	0.87 (±0.06)	0.99
K	Initial	46.5 (±2.13)	0.15 (±0.02)	0.99	48.8 (±2.19)	0.12 (±0.02)	0.99
	1 hour	81.4 (±8.51)	0.29 (±0.05)	0.97	89.6 (±8.67)	0.30 (±0.05)	0.97
	6 hour	145 (±11.3)	0.30 (±0.04)	0.98	245 (±5.60)	0.16 (±0.01)	1.00
	24 hour	288 (±7.65)	0.24 (±0.01)	1.00	302 (±7.21)	0.22 (±0.01)	1.00
Mg	Initial	9.17 (±2.40)	0.55 (±0.11)	0.94	11.4 (±3.67)	0.49 (±0.14)	0.88
	1 hour	9.09 (±3.81)	0.92 (±0.17)	0.96	13.0 (±3.84)	1.04 (±0.11)	0.98
	6 hour	3.60 (±0.38)	1.17 (±0.04)	1.00	22.3 (±6.56)	1.13 (±0.11)	0.99
	24 hour	13.5 (±3.32)	0.72 (±0.10)	0.97	13.7 (±1.09)	1.37 (±0.03)	1.00

Si was initially preferentially released compared to Mg for both solutions (*Figure 5.4a*) with dissolution becoming near congruent by 16 days of dissolution in deionised water. For acid solutions, Mg/Si increased with milling and dissolution times with all three milled samples showing relatively greater dissolution of Mg for dissolution times greater than 2 days (*Figure 5.4a*) or more than 2% of the mineral dissolved (*Figure 5.4b*).

These results for Mg and Si dissolution of milled biotite in acid solution are consistent with those reported by Acker and Bricker (1992) and Turpault and Trotignon (1994), with both reporting the greater release of Mg than of Si from biotite although Mg/Si congruency develops for greater percent dissolution for all milling times (*Figure 5.4b*). Turpault and Trotignon (1994) proposed that alteration progresses rapidly from crystal edges with minimal alteration of the basal surface. TEM images of pre-dissolution B24 (*Figure 5.5*) show the presence of thin, lathlike particles of biotite with the longest edge being less than 100nm and with a large edge to surface area ratio, allowing for rapid dissolution of Mg by dissolution from edge sites. The dissolved Mg/Si ratio is pH dependent, with higher Mg/Si ratios occurring at pH 4.5 compared with near congruent dissolution at pH 5.5 in deionised water, and a Mg reaction order for B24 greater than 1. In addition, the Si concentrations of B24 were also less than that of B1 and B6 for both solutions (*Figure 5.3*) possibly

indicating the reduced dissolution of the basal surface of ultrafine particles, with corresponding increase of edge weathering. Holdren and Speyer (1985b; 1987) proposed that dissolution is dependent on the distance between dislocations. Where grain size is the same as the distance between dislocations, then surface area no longer influences mineral dissolution as additional surface defects are not produced, regardless of increasing surface area. Milled biotite may have reached a particle size that corresponds to this criterion. Hodson (1999) also proposed that the movement of solutes within microcracks might affect dissolution rates where dissolution rates are transport limited.

Hornblende

Concentrations of Si, Ca and Mg were greater in the acid solution than the deionised water solutions (*Figure 5.6*). This can be attributed to the pH in the deionised water (≈ 8) that supported lower dissolution rates than acid solutions and is in accordance with other dissolution studies using this hornblende (Sverdrup, 1990). Concentrations increased with milling time for all elements. Si dissolution reaction order (*Table 5.3*) increased from near parabolic ($n \approx 0.5$) for H0 to near linear ($n \approx 1$) for H1 for both solutions. Linear kinetics also applied for Si dissolution from H6 and H24 in acid solution while dissolution of these samples in deionised water was best described by a near parabolic reaction order. Ca reaction order increased for all milling times compared with the unmilled minerals with the highest value being 0.5 for deionised water and 0.6 for acid solution. Differences in the n for milled hornblende may not be statistically significant. Mg reaction order increased with milling time from ≈ 0.5 for H0 to ≈1 for milled samples, with H24 approximating 1.4 in acid solution. This latter value is similar to the reaction order of B24 in acid solutions, again suggesting that the octahedral layer of highly milled amphiboles is readily dissolved in acid solution.

The initial dissolution of milled hornblende (H1, H6, H24) was characterised by rapid Ca release relative to Si over the first 4 days in both solutions, followed by decreasing Ca/Si ratios (*Figure 5.7a*). Conversely, Mg/Si increased during the first 4 days of dissolution, and continued to increase slightly during ongoing dissolution, although decreasing for dissolution of H0. The near linear reaction order of both Si and Mg dissolution is associated with the near steady-state stoichiometric dissolution of these elements after approximately 4% of the mineral had dissolved (*Figure 5.7b*).

Table 5.3: Value of coefficients a (μmoles g^{-1}) and n of the power equation fitted to the relationship between cumulative element release and dissolution time for milled hornblende in deionised water and acid (pH 4.5) solutions. Values in brackets are the standard errors of the coefficients.

Element	Milling Time	Deionised Water			pH 4.5		
		a	*n*	R^2	*a*	*n*	R^2
Si	Initial	14.5 (±1.99)	0.62 (±0.06)	0.99	18.7 (±1.25)	0.52 (±0.03)	0.99
	1 hour	23.8 (±4.97)	0.86 (±0.08)	0.99	32.6 (±11.6)	0.85 (±0.14)	0.96
	6 hour	45.6 (±12.8)	0.65 (±0.12)	0.95	33.0 (±7.78)	1.08 (±0.09)	0.99
	24 hour	46.0 (±11.5)	0.61 (±0.10)	0.95	42.3 (±6.40)	1.02 (±0.06)	1.00
Ca	Initial	10.8 (±1.22)	0.34 (±0.05)	0.97	15.3 (±1.50)	0.23 (±0.05)	0.96
	1 hour	27.6 (±4.46)	0.48 (±0.07)	0.97	34.2 (±6.77)	0.48 (±0.09)	0.95
	6 hour	56.7 (±20.3)	0.45 (±0.16)	0.84	57.1 (±9.09)	0.63 (±0.07)	0.98
	24 hour	66.4 (±19.6)	0.47 (±0.13)	0.89	87.1 (±25.4)	0.65 (±0.12)	0.95
Mg	Initial	12.8 (±2.23)	0.43 (±0.08)	0.95	11.4 (±3.67)	0.49 (±0.14)	0.88
	1 hour	21.9 (±5.96)	0.77 (±0.11)	0.98	13.0 (±3.84)	1.04 (±0.11)	0.98
	6 hour	22.0 (±11.0)	1.08 (±0.19)	0.96	22.3 (±6.56)	1.13 (±0.11)	0.99
	24 hour	23.7 (±8.64)	1.10 (±0.14)	0.98	13.7 (±1.08)	1.37 (±0.03)	0.99

5.3.2 Mineral Dissolution Rates and Reactive Site Distribution

Unit mass dissolution rates are presented in *Figures 5.8* to *5.10* as functions of dissolution time. Dissolution rates for unmilled minerals and minerals milled for 1 hour all decreased with time. Various trend in dissolution rate were observed for minerals milled for 6 and 24 hours, with the dissolution rate of some elements increasing with time. Increasing dissolution rates with time were observed for:

- Si dissolution from M6 and M24 in both solutions;
- K dissolution from M6 in acid solution;
- Mg dissolution from B6 and B24 in both solutions;
- Si dissolution from H6 and H24 in acid solution; and
- Mg dissolution from H6 and H24 in both solutions.

Dissolution rates were higher in acid solution than in deionised water and generally increased with milling time except for:

- K dissolution from microcline in acid solution;

- K dissolution from biotite in both solutions;
- Si dissolution from biotite in both solutions;
- Si dissolution from hornblende in deionised water.

Decreasing dissolution rate with time has been attributed to the initial rapid dissolution of areas of dislocations and microtextures (Lee and Parsons, 1995) as well as to rapid dissolution of ultrafine particles (Zhang et al., 1993). Such arguments may be appropriate to explain dissolution of the unmilled minerals and minerals milled for 1 hour. The increasing dissolution rates of some elements with dissolution time indicate though that these points of initiation for mineral dissolution contribute to ongoing dissolution as the reaction proceeds.

The dissolution rate of a bulk solid is usually assumed to be proportional to its surface area (Banfield and Hamers, 1997) and the milled minerals used in this experiment have specific surface areas (*S*) as determined by BET adsorption ranging from approximately 3 m^2 g^{-1} for all unmilled minerals to approximately 60 m^2 g^{-1} for microcline, 135 m^2 g^{-1} for biotite and 170 m^2 g^{-1} for hornblende (*Table 4.1*). These values are much greater than are generally reported in dissolution studies and provide an opportunity to evaluate the influence of mineral surface area on mineral dissolution of ultrafine particles.

Values for coefficient *a* (*Table 5.1, 5.2* and *5.3*) generally increased with increasing milling time, and thus with increasing specific surface area (*S*). Thus plots of coefficicient a for all three minerals versus *S* have a positive slope for Si, K and Ca in both solutions, and Na dissolution in the acid solution (*Figure 5.11*). Where clear linear relationships were attained for both solutions, the slope of the regression line was greater for acid solution than for deionised water. The regression lines for Si are similar for all three minerals so the data are combined in *Figure 5.11*, which indicates that surface area may be more important than mineralogy in determining Si dissolution. Si is a good indicator of mineral dissolution rate due to it being part of the mineral framework (Oelkers, 2001) and not being a potentially exchangeable cation, such as K in biotite.

No single relationship between *a* and *S* existed for Mg dissolution data or when individual minerals were considered separately, suggesting that factors other than *S* influence dissolution of Mg from milled minerals. Several authors have suggested that the morphology of the mineral surface area described by geometric surface area (*s*) (Gautier et

al., 2001) or surface roughness (λ) (Anbeek, 1992b; Brantley et al., 1999; Lee and Parsons, 1995) maybe a better predictor of surface dissolution. Measurements of grain size and shape can be used to calculate *s* (Lee and Parsons, 1995) using *Equation 4.1* from the median particle size of the milled minerals determined by laser light scattering (LLS) and transmission electron microscopy (TEM) (*Table 5.3*).

Surface roughness is the relationship between *S* and *s* where:

$$\lambda = S/s \qquad \textit{Equation 5.3}$$

Thus we can calculate λ by LLS (λ_{LLS}) and TEM (λ_{TEM}) (*Table 5.4*). Although prediction of Mg dissolution in acid solution was possible using λ_{TEM} (*Figure 5.12*), Mg or Na dissolution in deionised water were not related to λ_{TEM} or λ_{LLS}. This would suggest that factors other than surface reactions are influencing the dissolution of Mg especially. TEM micrographs of both hornblende and biotite show aggregation of milled minerals (*Figures 4.10* and *4.12*). This aggregation may occur at points of charge in the octahedral layer exposed by milling, which may in turn influence dissolution of this layer.

Table 5.4: Values of specific surface area determined by BET measurements (S), geometric surface area calculated from median grain size by LLS (s_{LLS}) and TEM (s_{TEM}), and surface roughness calculated from LLS (λ_{LLS}) and TEM (λ_{TEM}).

Mineral	Milling Time	S ($g\ m^{-2}$)	s_{LLS} ($g\ m^{-2}$)	s_{TEM} ($g\ m^{-2}$)	λ_{LLS}	λ_{TEM}
Microcline	Initial	3.9	0.24	3.10	16.0	1.26
	1 hour	9.3	0.31	3.51	30.4	2.65
	6 hour	34	0.23	5.88	147	5.78
	24 hour	59	0.38	4.71	155	12.5
Biotite	Initial	3.6	0.05	1.18	68.8	3.06
	1 hour	31	0.24	1.53	131	20.3
	6 hour	99	0.34	4.08	288	24.3
	24 hour	135	0.28	8.00	479	16.9
Hornblende	Initial	2.8	0.22	1.88	12.5	1.49
	1 hour	20	0.43	1.27	46.2	15.8
	6 hour	101	0.30	1.67	339	60.3
	24 hour	169	0.42	9.38	403	18.0

5.3.3 Limitations of Methodology

Values of solution pH of the bulk solution outside the dialysis tubing were similar to those in the dialysis tubing at the completion of experiment *(Figures 5.13, 5.14* and *5.15*), indicating free movement of protons between the two solutions. Final element concentrations differed between the two solutions with no single trend being observed. Larger differences in elemental concentrations occurred for the deionised water solution than the acid solutions, especially for biotite and hornblende. In general, element concentrations were higher in the solution in the dialysis tubing than in the bulk solution, especially for deionised water. This difference presumably represents the role of the dialysis membrane in restricting rapid transfer of ions between the solutions.

The dissolution experiment was originally designed for 64 days of dissolution to enable substantial dissolution of the minerals and thus provide an estimate of longer-term dissolution kinetics of the milled minerals. Leaking by some of the dialysis tubing, however, shortened the experiment and introduced potential contamination of some of the bulk solutions by mineral particles. Of greater concern, however, is the substantial differences in final concentrations between the bulk solution and solution in the dialysis tubing, indicating that the membrane may be acting to reduce transfer to the bulk solution and thus potentially reducing the dissolution rate due to mass action consideration. These differences were not systematic and make interpretation of the results difficult. The limited agitation of mineral powders within the dialysis tubing may have resulted in diffusion-limiting conditions within the tubes (i.e. the ideal stirred condition was not achieved). The results of this study suggest that the use of dialysis tubing as described here has the potential for use in dissolution studies of ultrafine particles but that the method requires further evaluation and development. Modification of the method to ensure adequate mixing without leaking and to ensure adequate reaction time for steady state conditions to be achieved is required. Alternatively, Eick et al. (1996) describe a method for dissolution experiments involving ground basalt where the solids were allowed to settle for two hours prior to collection. The reacting solution was then drawn from the top of the solution column and the sample filtered through a 0.20 μm filter. Adoption of such a procedure may overcome some of the limitations of the current experiment.

Only Si, K, Na, Mg and Ca were determined during this experiment as these elements were most important in relation to the ultimate purpose of this work – the use of milled silicate

minerals as fertilisers. Information regarding the release of other elements, especially Al and Fe would have aided in interpretation of the congruency of dissolution and allowed for solubility calculations. Similarly, titration of H^+ while maintaining the pH of the acid solution could have been used for predicting acid neutralizing values.

5.3.4 Implications for the Use of Milled Minerals and Rocks as Fertilisers

The premise for undertaking attrition milling in order to improve the fertiliser effectiveness of silicate minerals is that dissolution of minerals will be enhanced by increasing the surface area and points of dissolution initiation. The results of this dissolution experiment indicate that attrition milling increases the dissolution rate of silicate minerals in aqueous solutions. An effective mineral fertiliser should have dissolution characteristics that will both supply immediate plant requirements in a growing season and provide a long-term source of nutrients over multiple growing seasons. The minerals used in this experiment showed major increases in the dissolution of several macronutrients (K, Ca, Mg, Na, Si) with attrition milling during both the initial (incongruent dissolution) and subsequent (more nearly congruent) dissolution phases. In all cases though, only a minor proportion of the mineral dissolved during the experiment. The tendency towards a reaction order of 1 with increasing milling indicates that ongoing dissolution will occur and continue to supply nutrients over a longer period of time.

The literature indicates that mineral dissolution rates may be 2-3 orders of magnitude less in the field than in laboratory experiments (White, 1995). However dissolution rates in soils may be increased if the soil provides a reservoir of H^+ and acts as sinks for solutes as soil constituents and plants remove elements from soil solution thereby contributing to further dissolution due to the mass action effect (Hinsinger et al., 2001).

Silicate mineral fertilisers have been examined as a potential source of K more than for any other nutrient (Bakken et al., 2000; Bolland and Baker, 2000; Coroneos et al., 1996; Weerasuriya et al., 1993). Granite and K-feldspars have been the main focus of research due to their abundance. Their effectiveness is however limited by their resistance to dissolution (Bolland and Baker, 2000) whereas biotite may be more effective as it releases interlayer K by exchange with no requirement for dissolution of the layer structure (Bakken et al., 2000). Attrition milling increased K release from both biotite and microcline, with K release from milled microcline being comparable to that from biotite.

The release of K from biotite may have, however, been restricted by the K concentration in solution (Springob, 1998). Attrition milling provides a technique whereby K from these normally unavailable sources may be released. Milling may also increase dissolution of muscovite, another potential K fertiliser (Kalinowski and Schweda, 1996; Nagy, 1995).

The increase in solution pH of deionised water that had reacted with ground minerals indicates the potential of silicate minerals to act as acid neutralizing agents for acid soils. Amphiboles in particular are considered important in proton neutralization in soils (Zhang and Bloom, 1999) and for CO_2 consumption (Berner, 1995). Attrition milling of minerals will increase their acid neutralizing value by accelerating reaction with soil acidity.

Reactive surface area as measured by the BET gas adsorption method is the best method for evaluating milling performance, and normalising dissolution data relative to the reactive surface area allows quantitative assessment of the influence of grain surface properties on nutrient release. Such results are important in the evaluation of the impact of milling on silicate mineral fertilisers and provide a basis to compare results from different minerals and experiments. Such an approach may also be of benefit in providing a unifying method by which plant growth experiments involving the application of silicate rocks and minerals can be compared.

5.4 Summary

The early, rapid dissolution of ultrafine silicate minerals with high surface areas (BET surface areas ranging from 2 to 169 $m^2\ g^{-1}$) was examined to evaluate these materials as potential sources of nutrients to plants. No pre-treatment to remove fine-grained material was undertaken of the highly milled microcline, biotite and hornblende prior to dissolution in deionised water and dilute HCl.

Changes in elemental concentrations of each mineral indicates the following trends:

1. **Microcline**

- Milling greatly (≈10-100x) increases the dissolution of microcline.
- The initial dissolution of microcline is incongruent but approaches congruency as 4% of the mineral dissolves.

2. **Biotite**

- Milling greatly (≈10-100x) increases the dissolution of Si and Mg from biotite. Mg/Si ratios indicate that congruent dissolution occurs after 1% of the mineral has dissolved.
- Similar increases in the release of K from biotite is due to release being by cation exchange, not only dissolution. This release is predominately instantaneous (≈ 1 day) then subsequent release is not greatly affected by milling. K release is initially noncongruent, approaching congruency by 4% dissolution. However, K/Si < 1 indicates that this is not truly congruent due to much of the initial loss of K by exchange.
- Milling of biotite produces lath-shaped particles with a greater percentage of edge area than for the original biotite that has mostly 00l face area. This allows for greater dissolution from the particle edges and subsequent preferential release of Mg.

3. **Hornblende**

- Milling greatly increased dissolution rate and solution pH.
- Dissolution of hornblende is probably congruent, although the low Ca/Si ratios in both deionised water and acid cannot be explained.

The dissolution rates of the minerals produced the following findings:

- Dissolution rates generally increased with milling time with minerals milled for 24 hours having dissolution rates greater than the initial milled minerals.
- Dissolution rates generally decreased with dissolution time and thus percent of the mineral dissolved.
- Dissolution rates in deionised water and acid are initially similar but by 16 days, dissolution rates in acid are approximately two times higher;
- Dissolution rates for biotite K are greatly reduced at 16 days of dissolution due to very rapid initial loss by exchange, which is then much restricted as K is not removed from solution.
- The increasing/asymptoting dissolution rates reflect reaction orders statistically equal to 1, i.e. linear dissolution, indicating those minerals will provide ongoing dissolution;

- Milling of biotite and hornblende for 24 hours sufficiently altered the octahedral layer of these minerals to allow for increasing dissolution rates with time.

Si, K and Ca dissolution rates were linearly related to specific surface area (determined by BET) for all minerals and both solutions, while Na dissolution from microcline was linearly related to specific surface area for the acid solution only. The relationship between Mg dissolution from biotite and hornblende was not linearly related to specific surface area, although a closer relationship was obtained when geometric surface area was used.

The agriculture benefits of increased silicate mineral dissolution via attrition milling require evaluation in plant growth experiments. Information is required on determining firstly the ability of this enhanced dissolution in supplying sufficient nutrients to sustain plant growth in the year of application, and secondly for ongoing supply in subsequent years. The influence of milled minerals on soil pH will also be of interest.

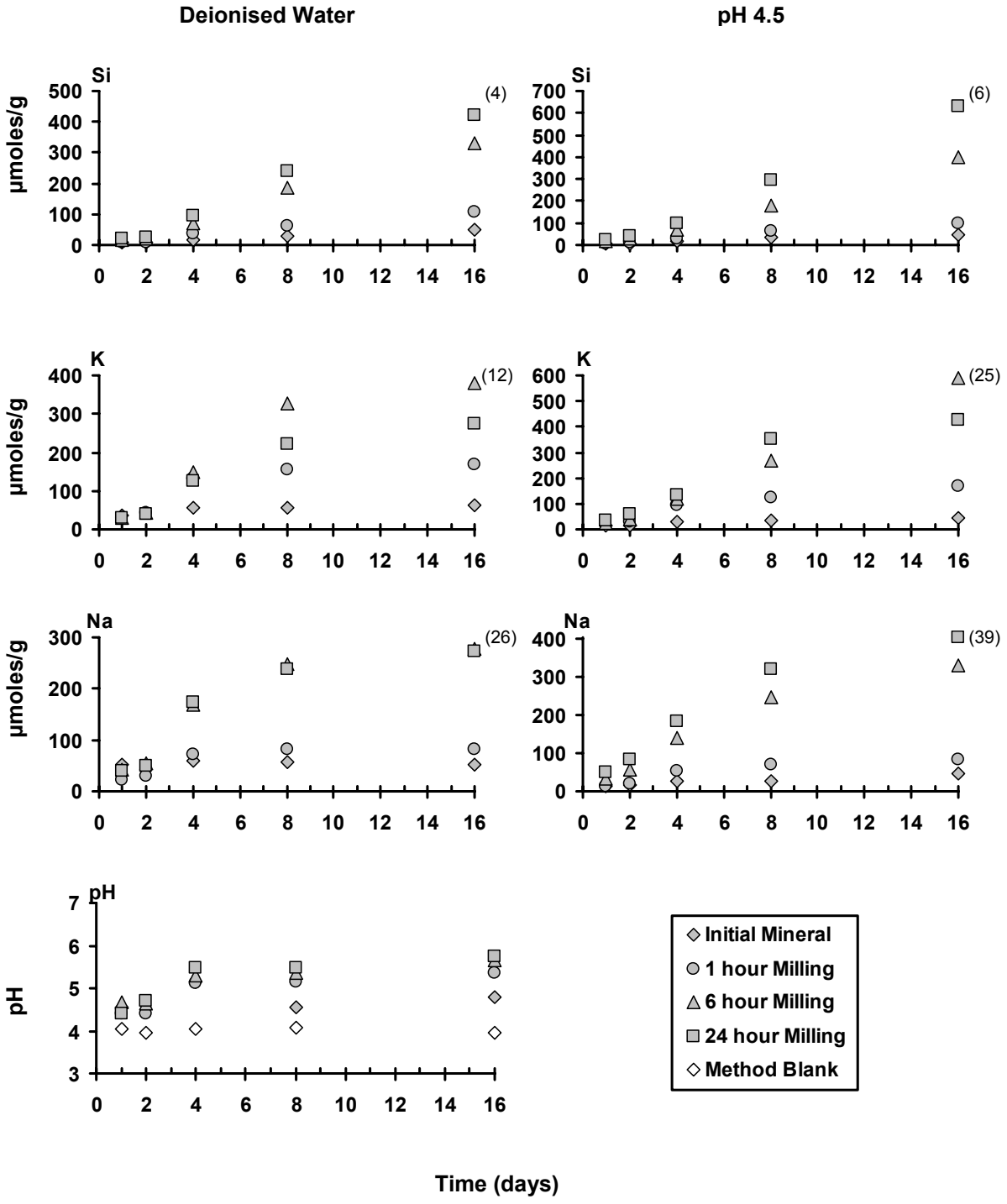

Figure 5.1: pH values in deionised water and Si, K and Na concentrations as functions of dissolution time for milled microcline in deionised water and acid (pH 4.5) solution. Values in parentheses are the largest percentage of mineral dissolved that is assumed to be the percentage of element dissolved.

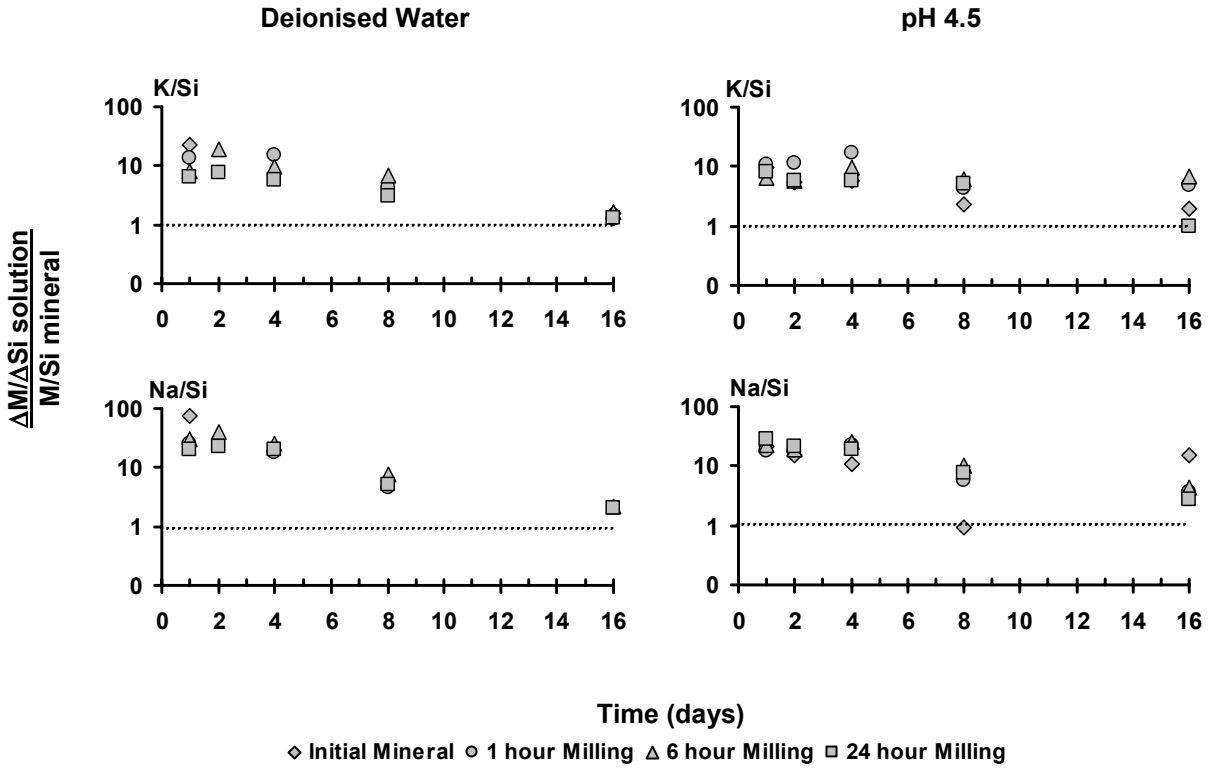

Figure 5.2a: Dissolution stoichiometry calculated from changes in solution concentrations for milled microcline normalised to the starting ratio of the mineral as a function of time for deionised water and acid (pH 4.5) solution. Dotted lines correspond to congruent dissolution.

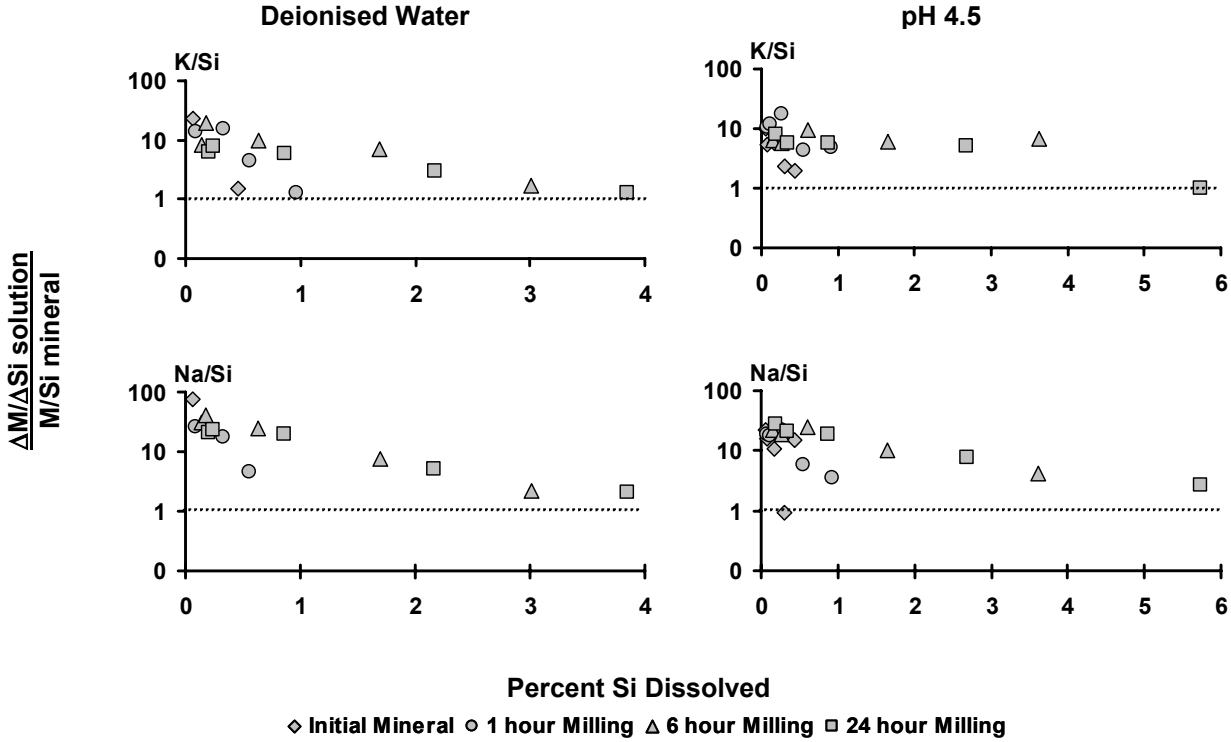

Figure 5.2b: Dissolution stoichiometry calculated from changes in solution concentration for milled microcline normalised to the starting ratio of the mineral as a function of percent Si dissolved in deionised water and acid (pH 4.5) solution. Dotted lines correspond to congruent dissolution.

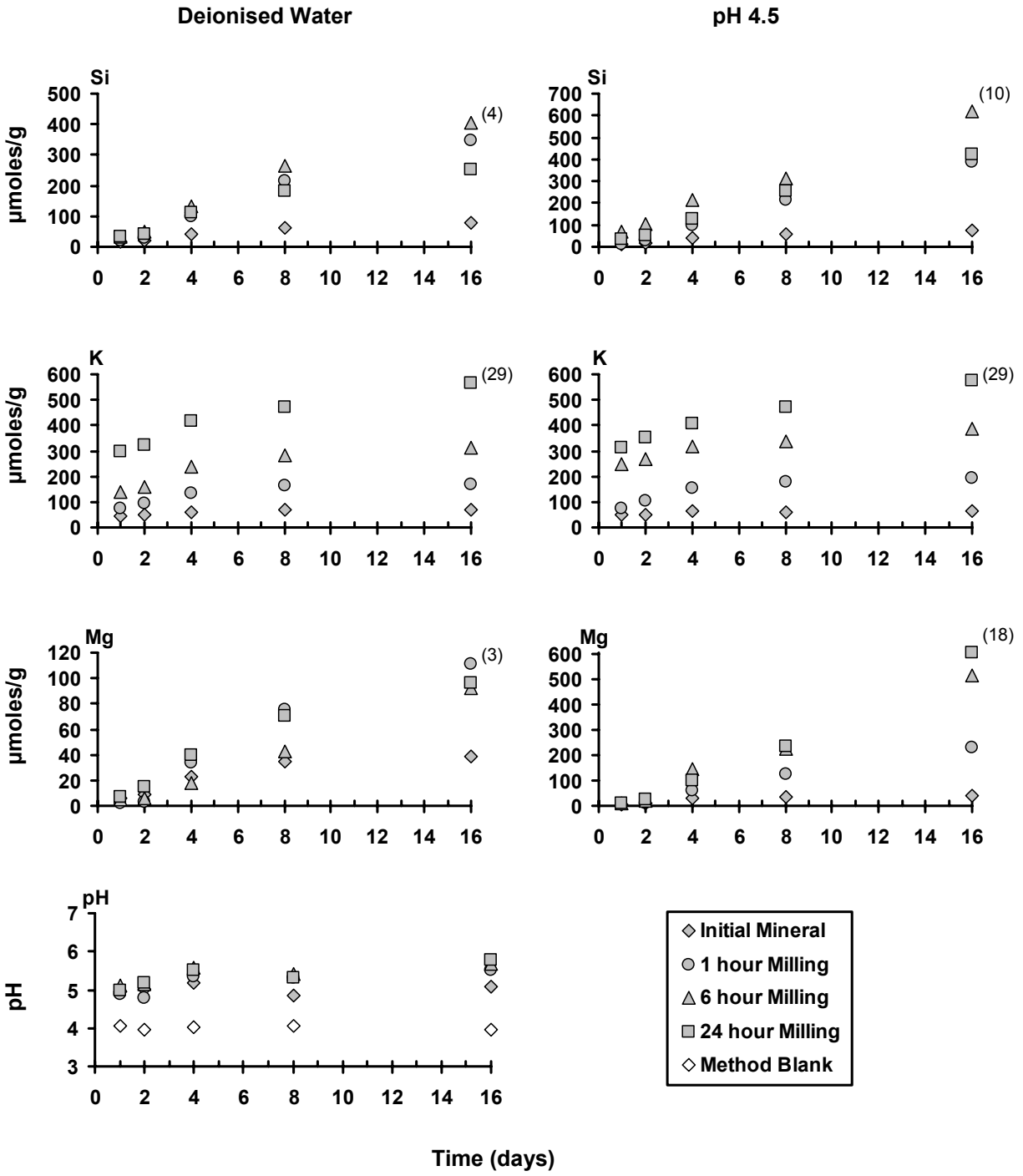

Figure 5.3: pH values in deionised water and Si, K and Mg concentrations as functions of dissolution time for milled biotite in water and acid (pH 4.5) solution. Values in parentheses are the largest percentage of mineral dissolved that is assumed to be the percentage of element dissolved.

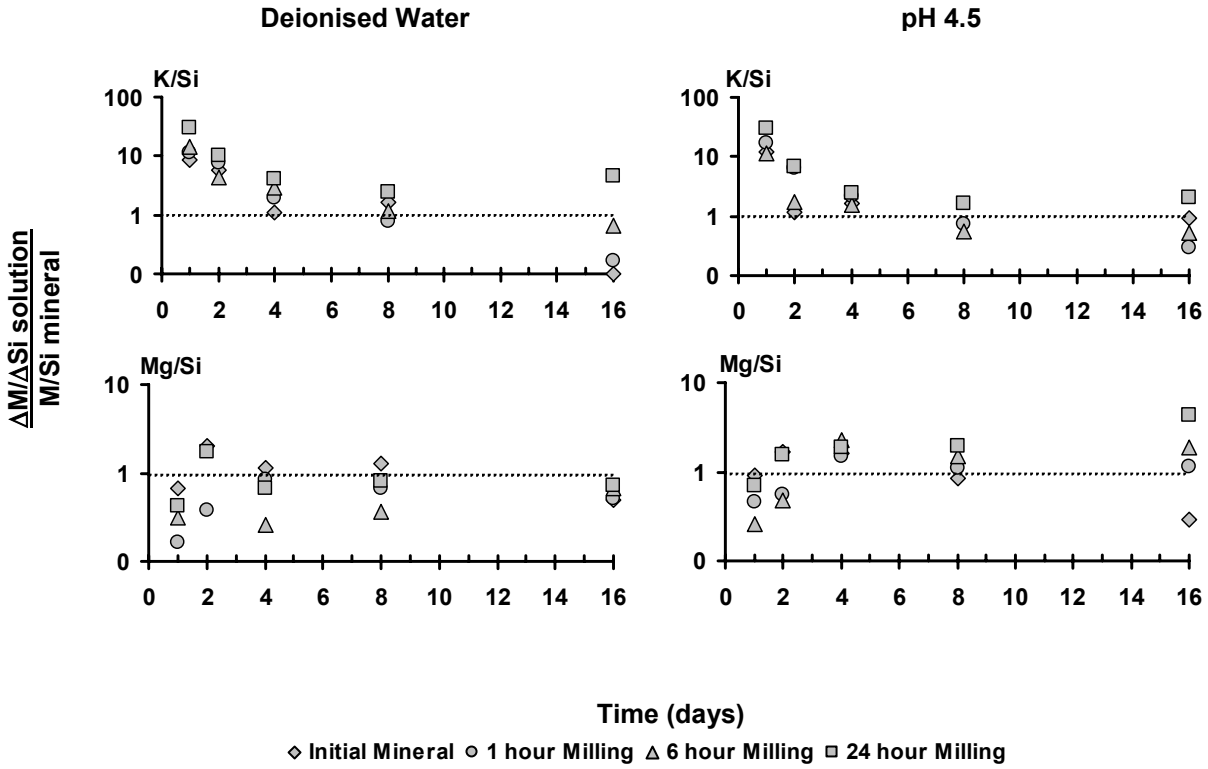

Figure 5.4a: Dissolution stoichiometry calculated from changes in solution concentration for milled biotite normalised to the starting ratio of the mineral as a function of time in deionised water and acid (pH 4.5) solution. Dotted lines correspond to congruent dissolution.

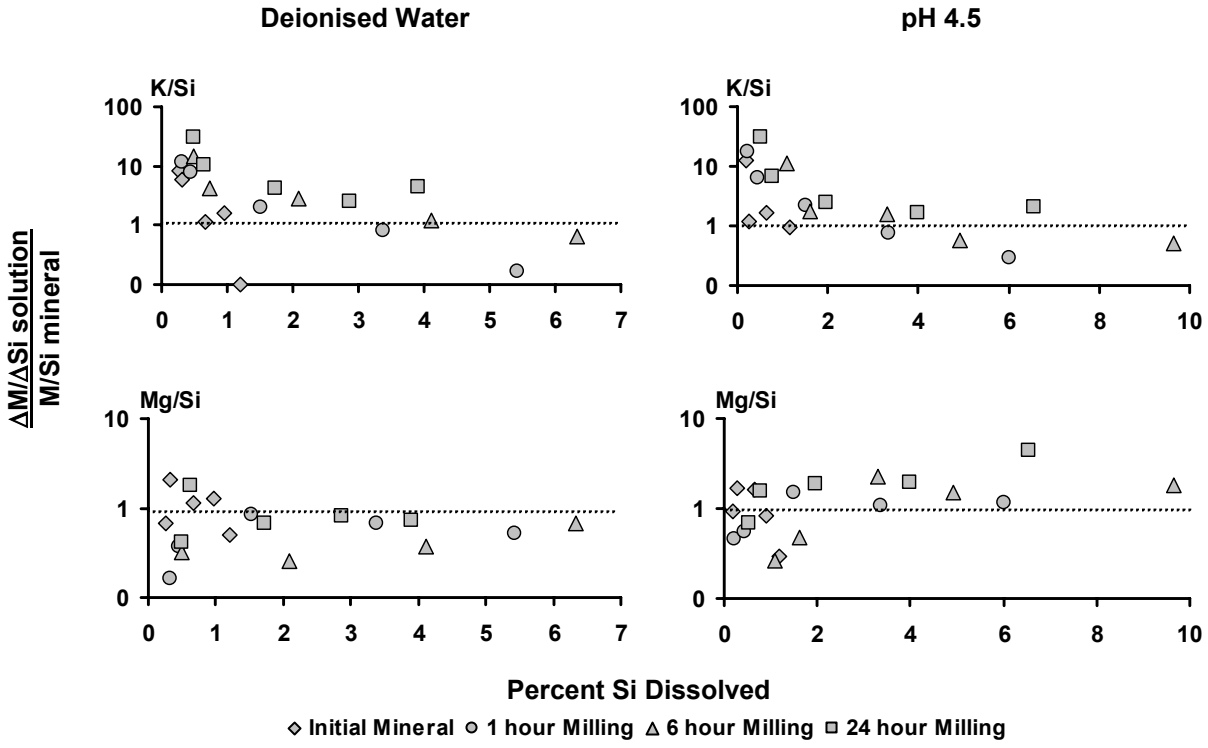

Figure 5.4b: Dissolution stoichiometry calculated by changes in solution concentration for milled biotite normalised to the starting ratio ofthe mineral as a function of percent Si dissolved in deionised water and acid (pH 4.5) solution. Dotted lines correspond to congruent dissolution.

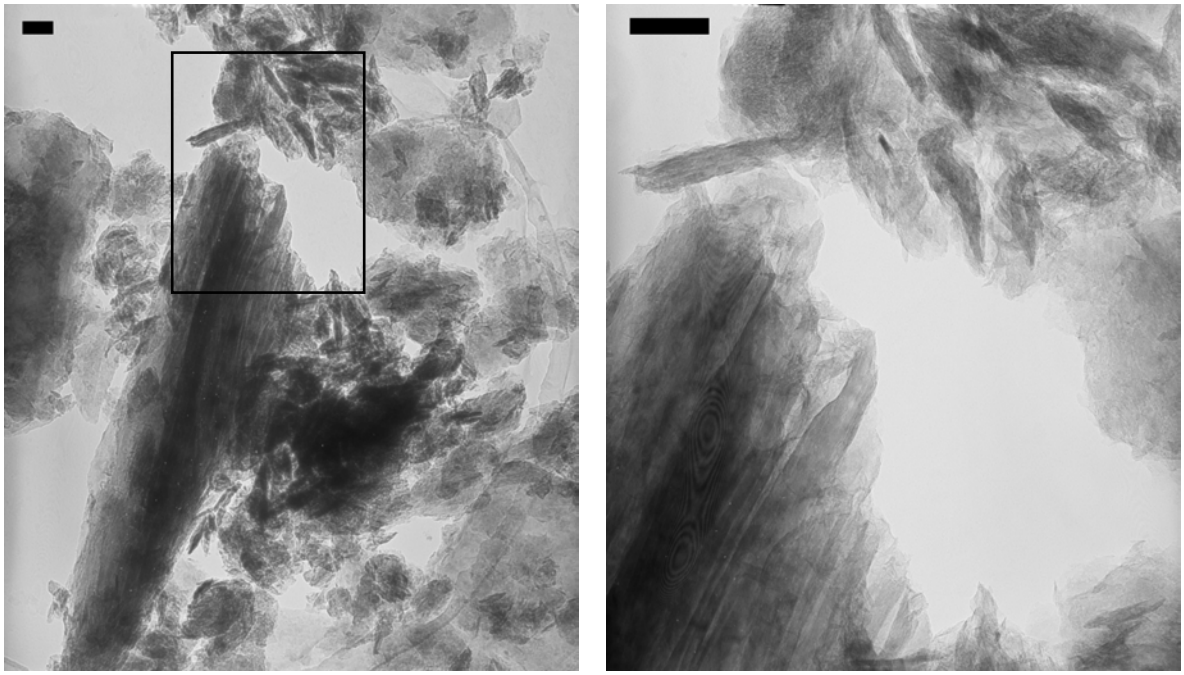

Figure 5.5: TEM micrographs of biotite milled for 24 hours prior to dissolution showing lathlike particles with large edge to surface area ratio. Image on right is an enlargement of the region defined by the box on the left hand micrograph. Scale bar is 100nm.

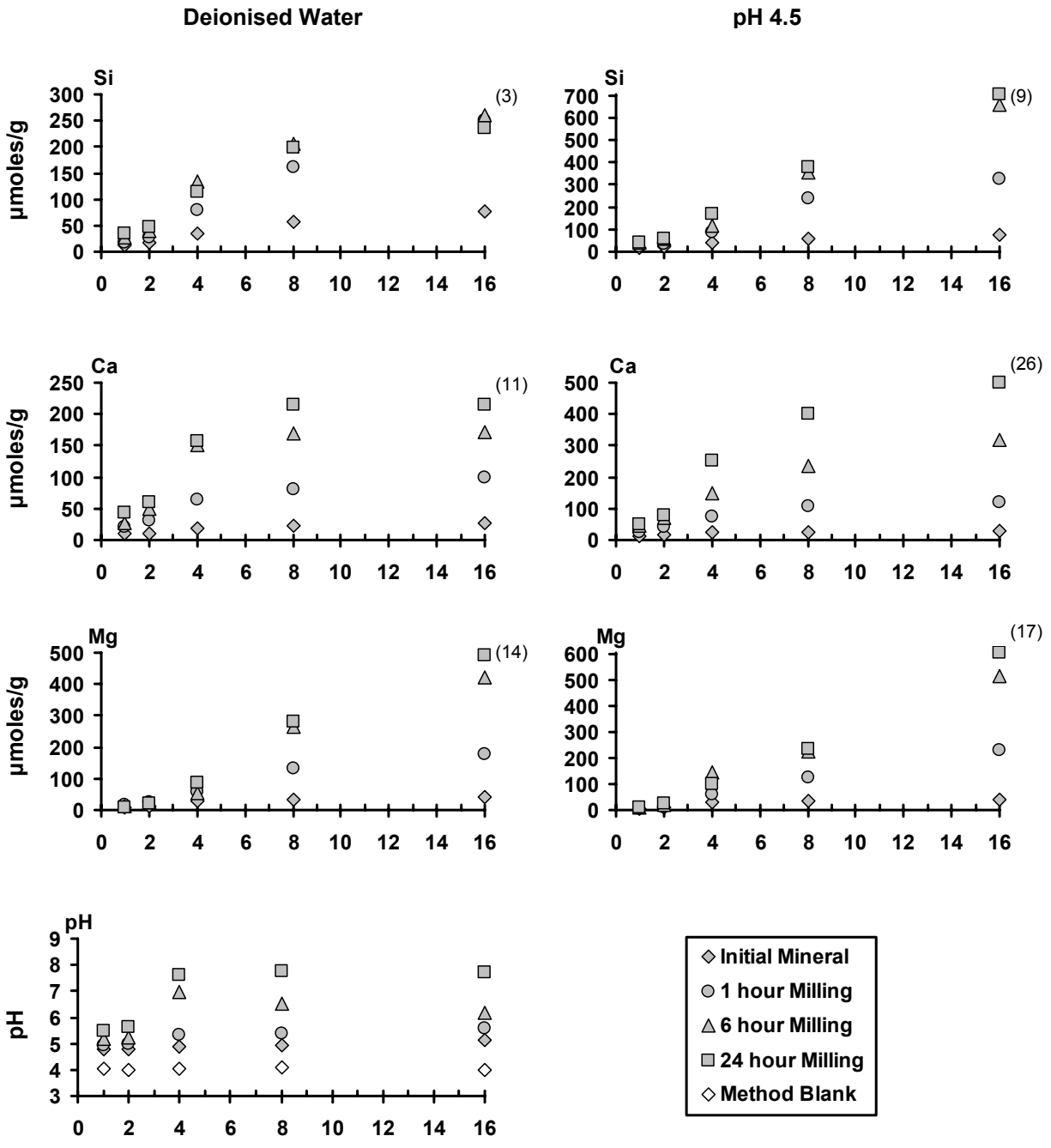

Figure 5.6: pH values in deionised water and Si, Ca and Mg concentrations as functions of dissolution time for milled hornblende in water and acid (pH 4.5) solution. Values in parentheses are the largest percentage of mineral dissolved that is assumed to be the percentage of element dissolved.

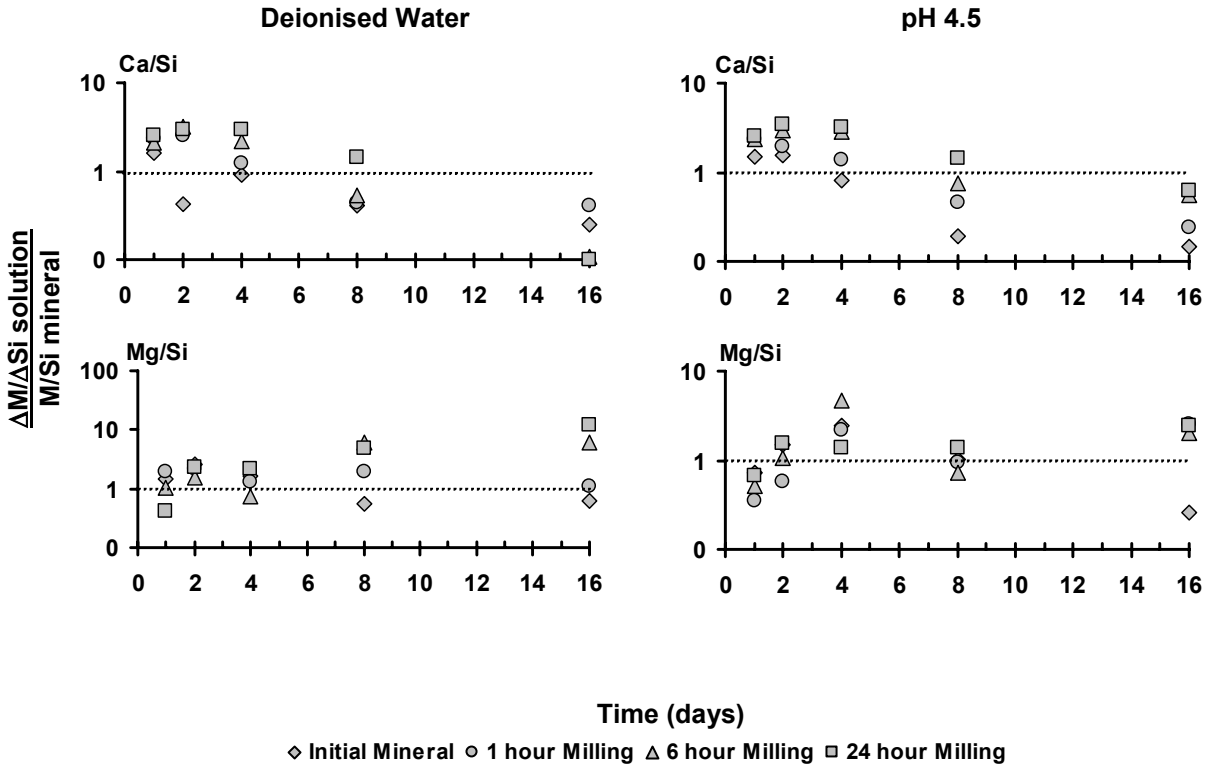

Figure 5.7a: Dissolution stoichiometry calculated from changes in solution concentration for milled hornblende normalised to the starting ratio of the mineral as a function of time for deionised water and acid (pH 4.5) solution. Dotted lines correspond to congruent dissolution.

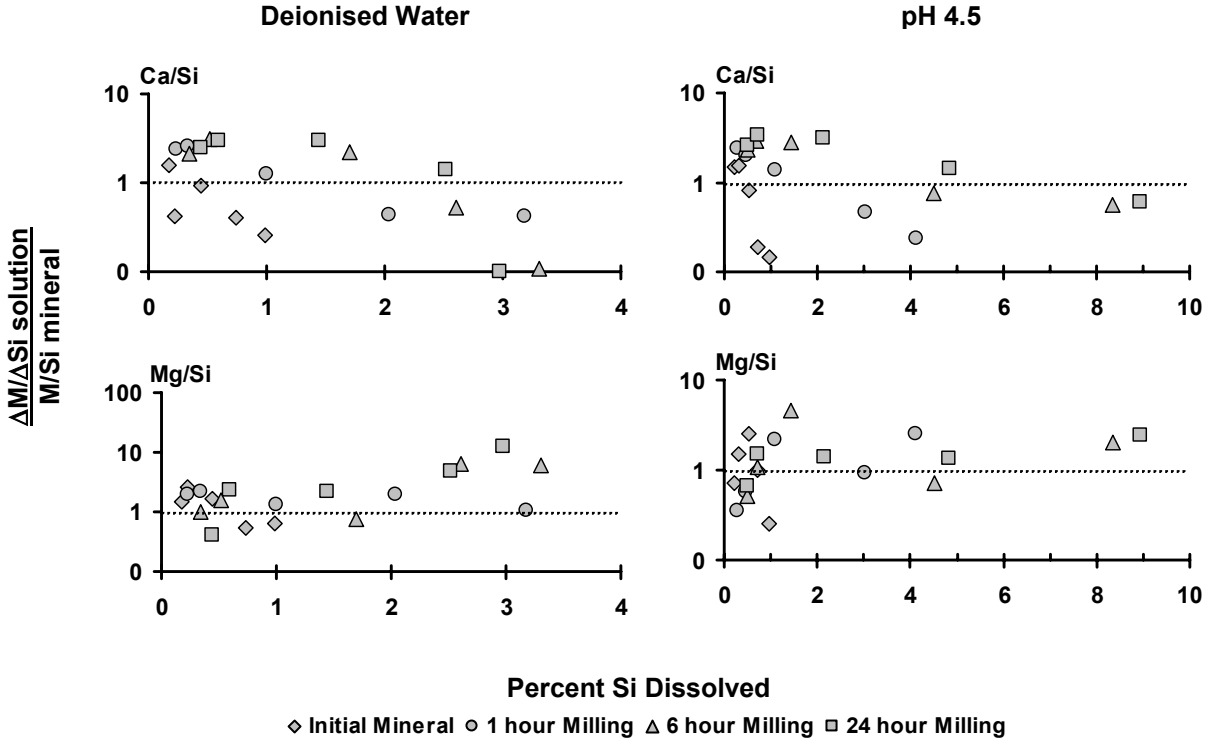

Figure 5.7b: Dissolution stoichiometry calculated from changes in solution concentration for milled hornblende normalised to the starting ratio of the mineral as a function of percent Si dissolved in deionised water and acid (pH 4.5) solution. Dotted lines correspond to congruent dissolution.

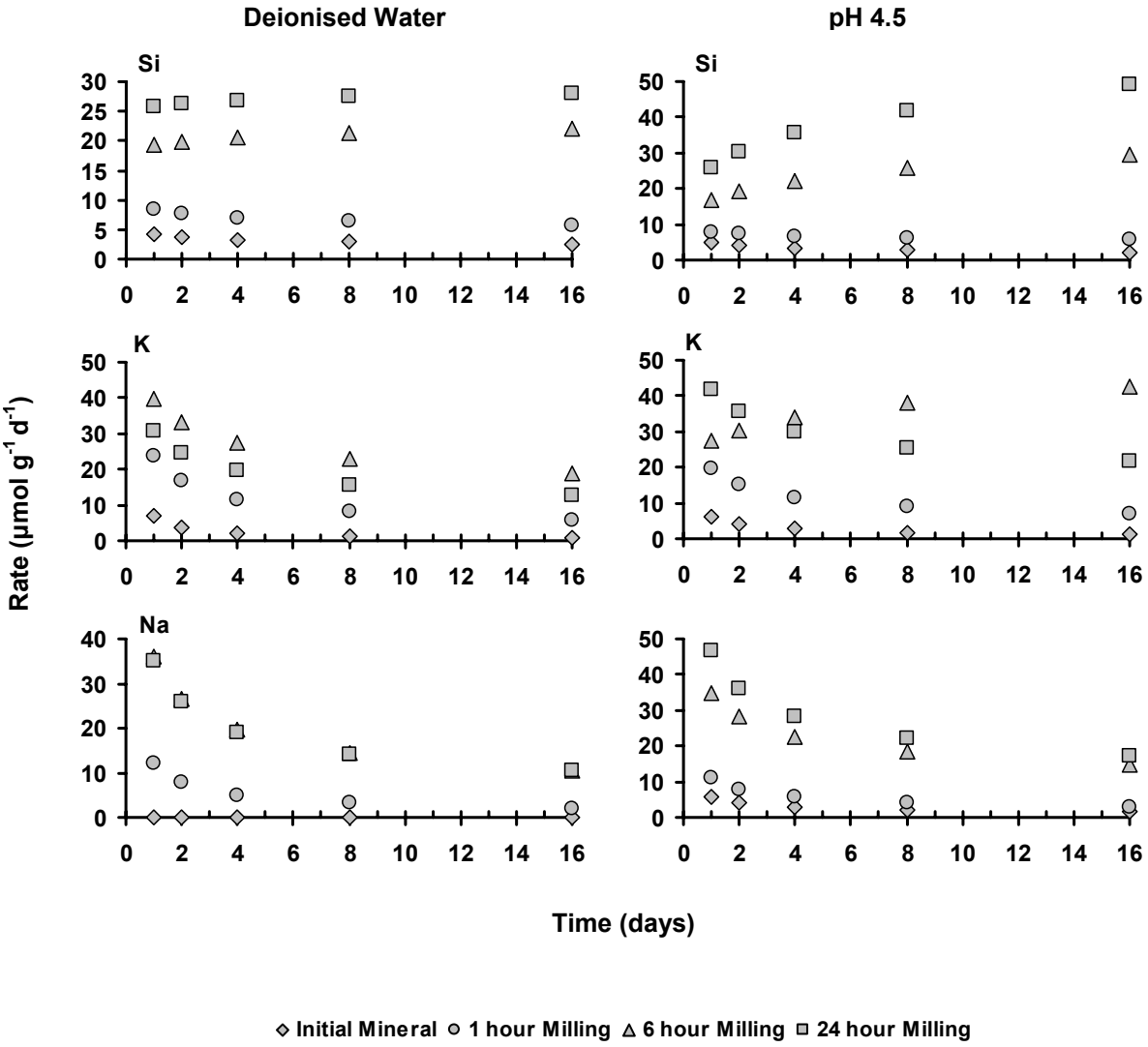

Figure 5.8: Dissolution rates for Si, K and Na calculated from the slope of the equation $E = aT^n$ as a function of time for milled microcline in deionised water and acid (pH 4.5) solution.

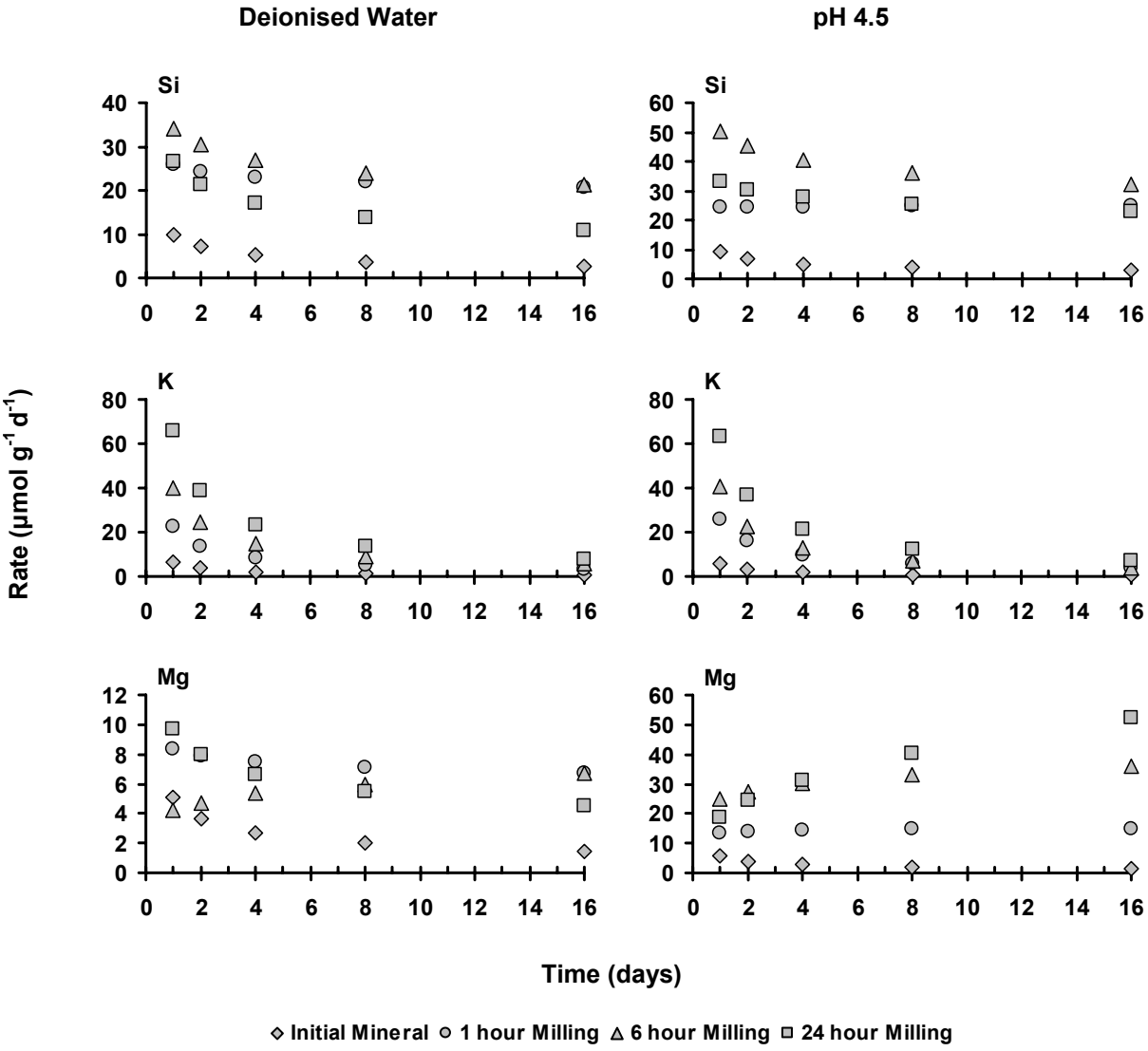

Figure 5.9: Dissolution rates for Si, K and Mg calculated from the slope of the equation $E = aT^n$ as a function of time for milled biotite in deionised water and acid (pH 4.5) solution.

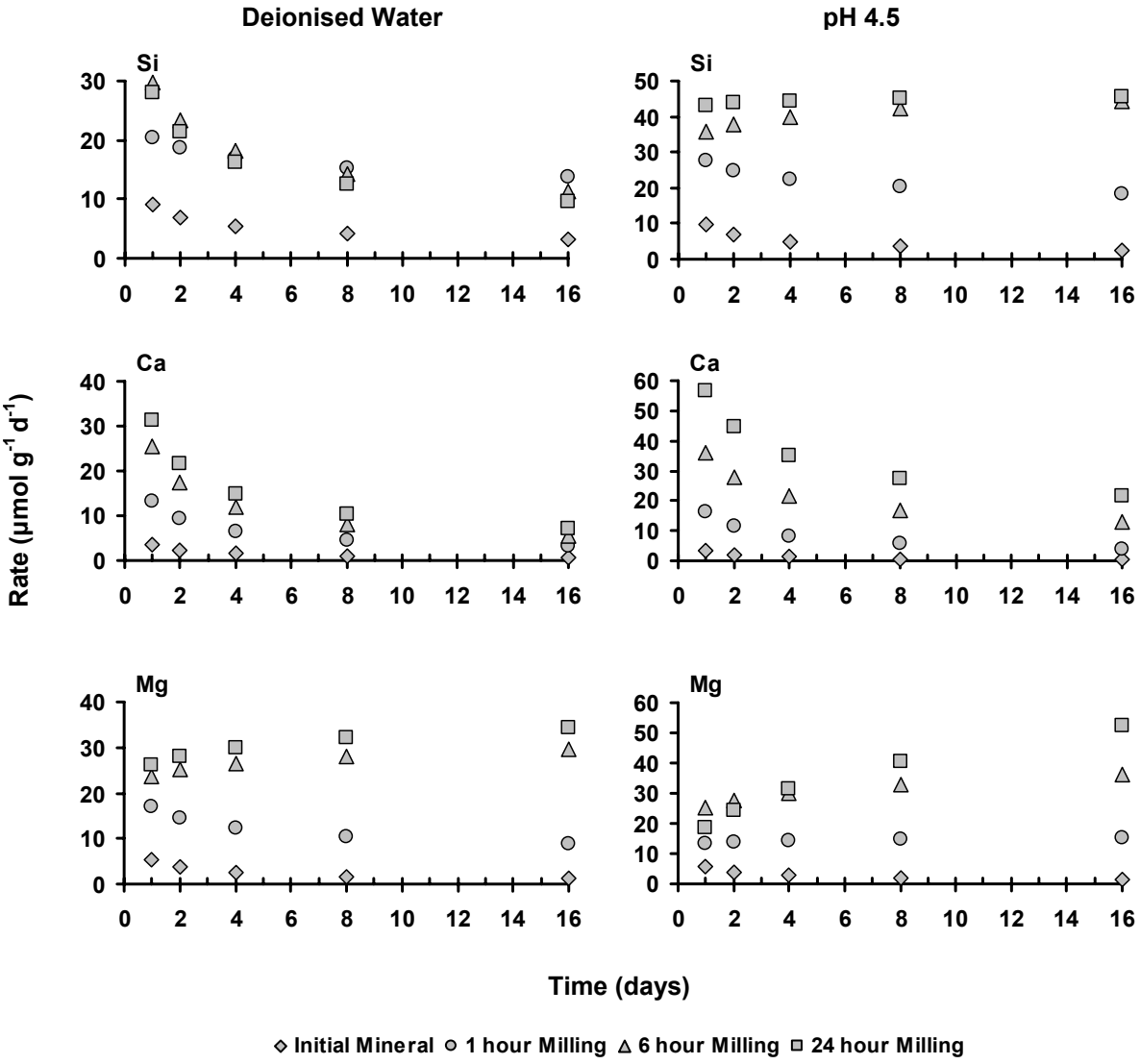

Figure 5.10: Dissolution rates for Si, Ca and Mg calculated from the slope of the equation $E = aT^n$ as a function of time for milled hornblende in deionised water and acid (pH 4.5) solution.

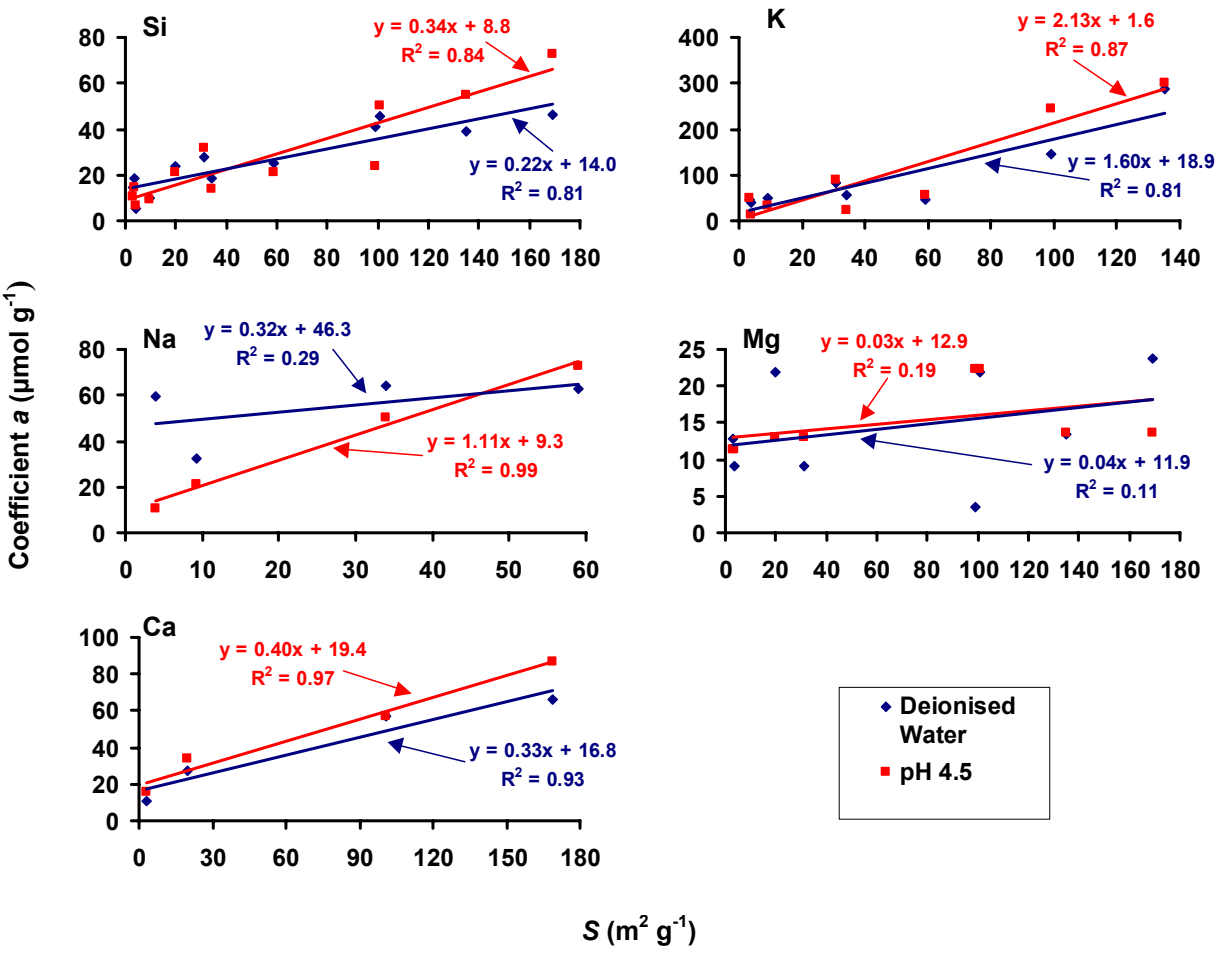

*Figure 5.11: Combined relationship between specific surface area (S) of all three minerals determined by the BET method and coefficient **a** calculated from dissolution curves (Tables 5.1, 5.2 and 5.3) for dissolution of the three milled minerals in deionised water and acid (pH 4.5) solutions.*

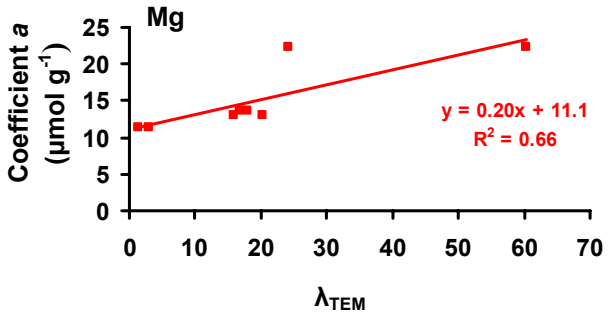

*Figure 5.12: Relationship between surface roughness calculated from BET and TEM measurements (λ_{TEM}) and coefficient **a** for Mg dissolution of milled biotite and hornblende in acid (pH 4.5) solution (Table 5.2 and 5.3).*

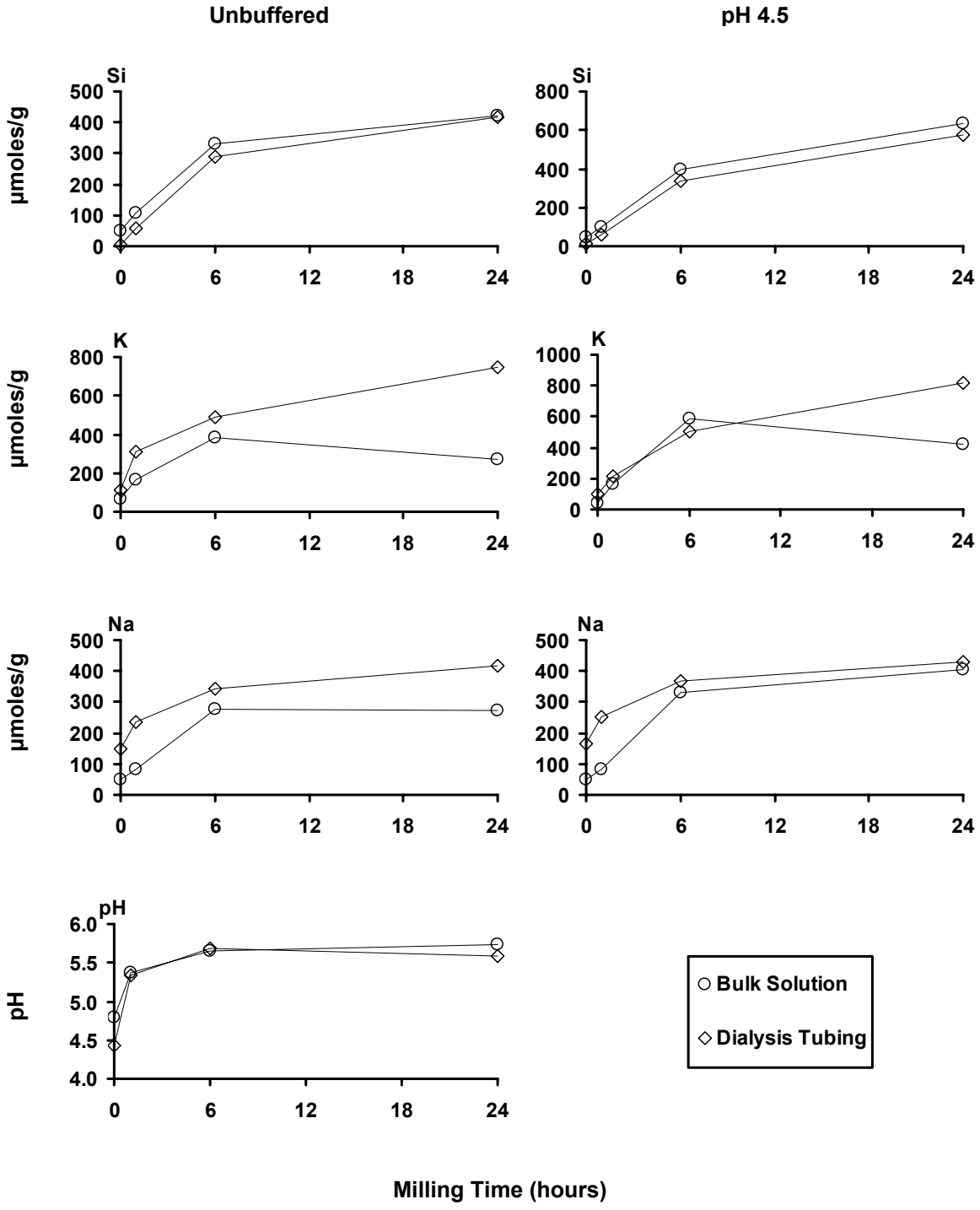

Figure 5.13: pH values of deionised water and Si, K and Na concentrations in bulk solution (outside dialysis tubing) and the solution inside the dialysis tubing as a function of milling time for dissolution of milled microcline in deionised water and acid (pH 4.5) solution for 16 days.

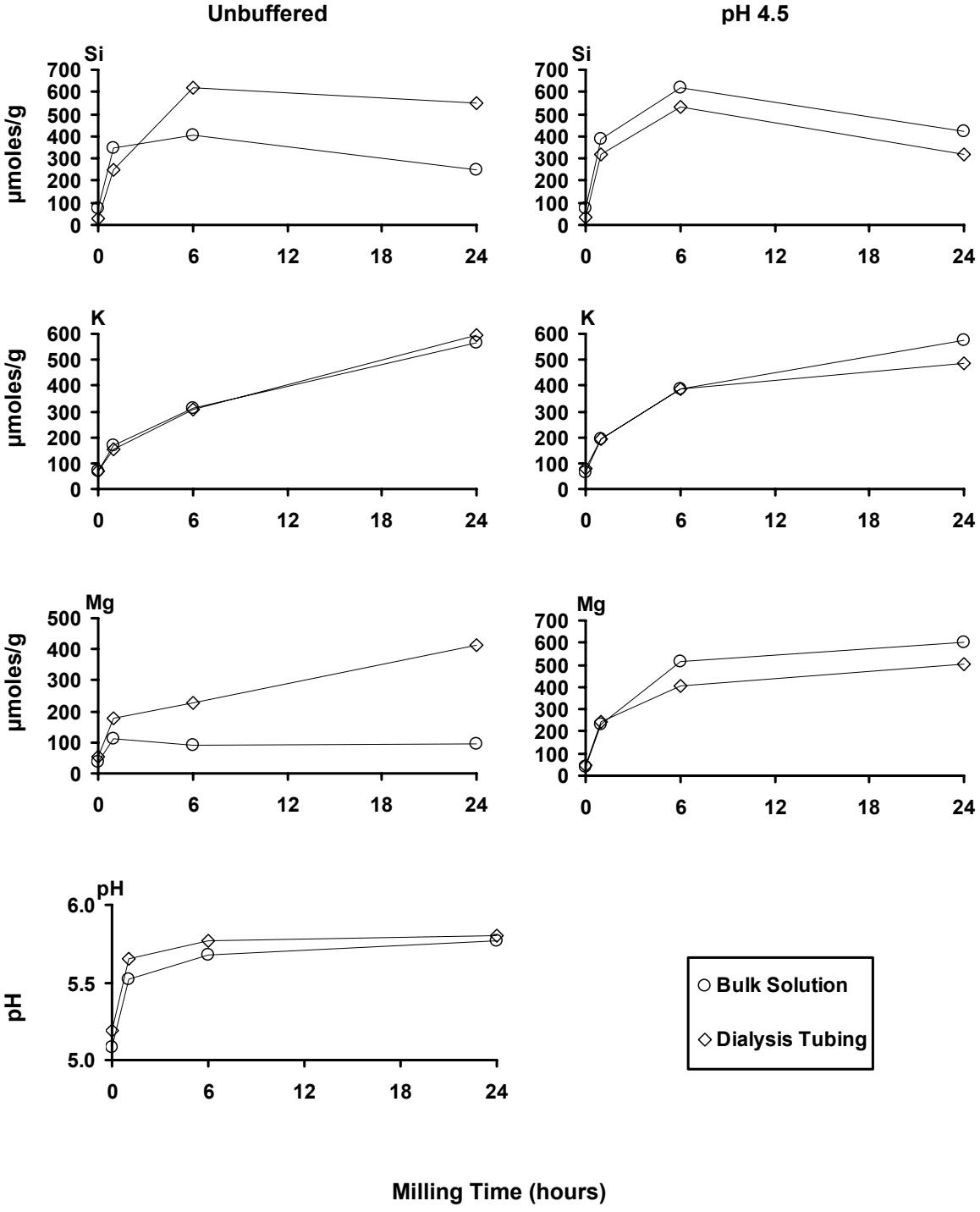

Figure 5.14: pH values of deionised water and Si, K and Mg concentrations in bulk solution (outside dialysis tubing) and the solution inside the dialysis tubing as a function of milling time for dissolution of milled biotite in deionised water and acid (pH 4.5) solution for 16 days.

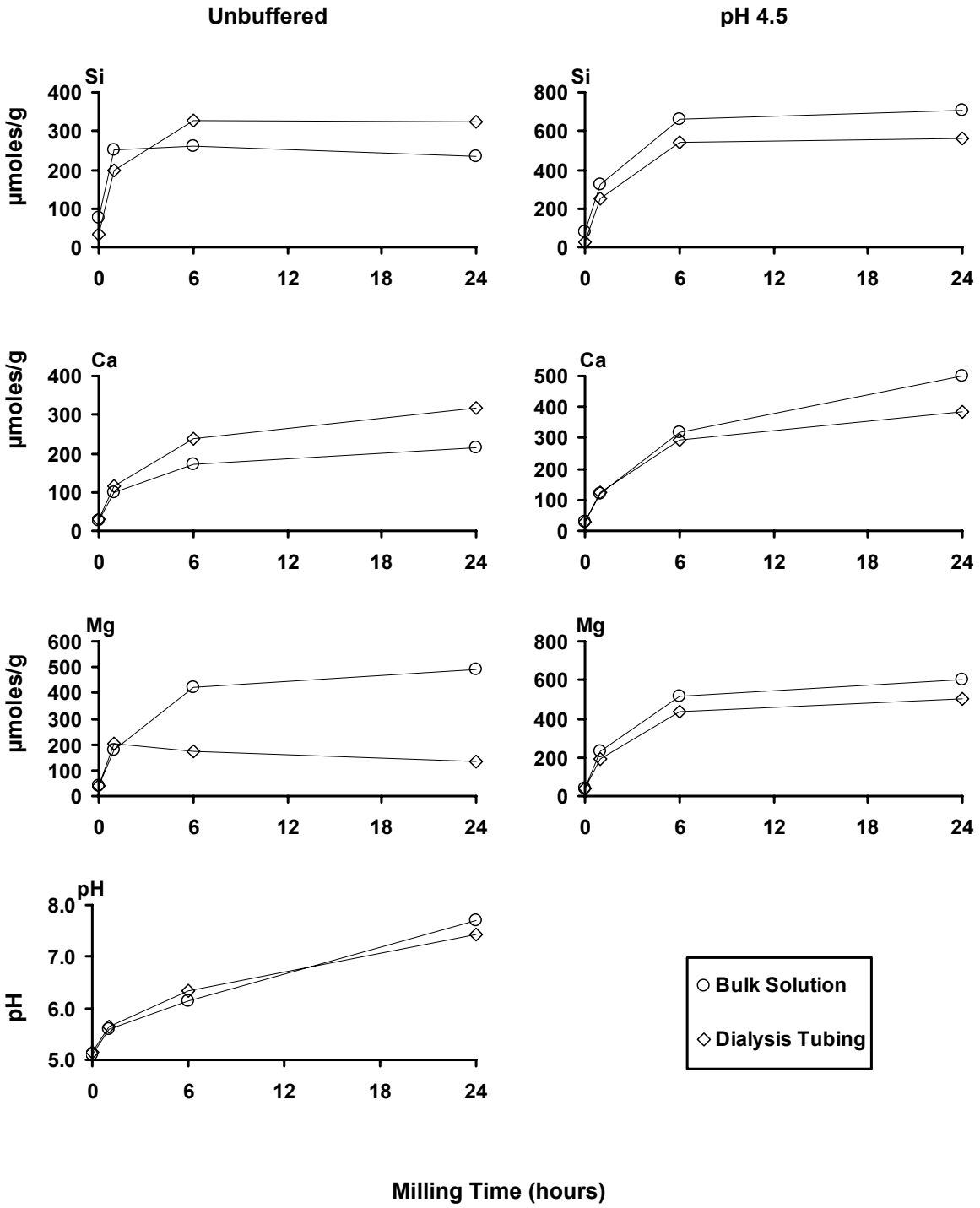

Figure 5.15: pH values of deionised water and Si, Ca and Mg concentrations in bulk solution (outside dialysis tubing) and the solution inside the dialysis tubing as a function of milling time for dissolution of milled hornblende in deionised water and acid (pH 4.5) solution for 16 days.